J|A|C|S
ARTICLES
Published on Web 04/09/2003

"Oscillating" Metallocene Catalysts: What Stops the Oscillation?

Vincenzo Busico,*,† Valeria Van Axel Castelli,† Paola Aprea,‡ Roberta Cipullo,‡ Annalaura Segre,§ Giovanni Talarico,‡ and Michele Vacatello‡

Contribution from the Dipartimento di Chimica, Università di Napoli "Federico II", Via Cintia, 80126 Naples, Italy, Istituto di Metodologie Chimiche, CNR, Area della Ricerca di Roma, 00016 Monterotondo Stazione, Italy, and Dutch Polymer Institute

Received September 7, 2002; E-mail: busico@chemistry.unina.it

Abstract: The 150 MHz ^{13}C NMR microstructural analysis of polypropylene samples produced with two representative "oscillating" metallocene catalysts of largely different steric hindrance, namely [(2-(3,5-di-*tert*-butyl-4-methoxyphenyl)indenyl)$_2$ZrP]$^+$ and [(2-phenylindenyl)$_2$ZrP]$^+$ (P = polymeryl), and the implications on the origin of the stereocontrol are presented and discussed in detail. The original mechanistic proposal of an "oscillation" between a *rac*-like (isotactic-selective) and a *meso*-like (nonstereoselective) conformation cannot explain the observed polymer configuration. The isotactic-stereoblock nature of the polymers obtained with the former catalyst proves unambiguously that the active cation "oscillates" between the two enantiomorphous *rac*-like conformations at an average frequency that, even at high propene concentration, is only slightly lower than that of monomer insertion. The less-hindered [(2-phenylindenyl)$_2$ZrP]$^+$ gives instead a largely stereoirregular polypropylene, which is the logical consequence of a faster ligand rotation; however, depending on the use conditions (in particular, on the nature of the cocatalyst and the polarity of the solvent), the polymerization products may also contain appreciable amounts of a fairly isotactic fraction. The peculiar microstructure of this fraction, with isotactic blocks *of the same relative configuration* spanned by very short atactic ones, rules out the possibility that the latter are due to an active species in *meso*-like conformation and points rather to a conformationally "locked" *rac*-like species with restricted ring mobility. The hypothesis of a stereorigidity induced by the proximity to a counteranion, which would play the role of the interannular bridge in the *rac*-bis(indenyl) *ansa*-metallocenes, was tested by computer modeling on a [*rac*-(2-phenylindenyl)$_2$ZrMe(C$_3$H$_6$)][B(C$_6$F$_5$)$_4$] ion couple and found viable.

Introduction

Of all metallocene-based propene polymerization catalysts,[1,2] the so-called "oscillating" ones are probably the most intriguing. Introduced in 1995 by Coates and Waymouth,[3] they owe the definition to the dynamic character of the active species, a cation of general formula [(2-Ar-indenyl)$_2$MtP]$^+$ (Mt = Zr or Hf; Ar = aryl; P = polymeryl).[4]

Stereorigid dimethylsilyl-*bridged* bis(2-phenyl-1-indenyl) zirconocenes in C_2-symmetric *rac* and C_s-symmetric *meso* configuration polymerize propene to site-controlled isotactic and atactic polypropylene, respectively.[4,5] The *unbridged* homologue gives instead a peculiar polypropylene which contains isotactic *and* atactic sequences and behaves as a thermoplastic elastomer.[3,4] This, and the observation of mixed "*rac*-like" and "*meso*-like" configurations in the crystal structure of the precursor (2-phenylindenyl)$_2$ZrCl$_2$, originally led the inventors to postulate that in solution the catalytic species "oscillates" between a "*rac*-like" (isotactic-selective) and a "*meso*-like" (nonstereoselective) conformation at a frequency intermediate between those of monomer insertion and chain transfer, with a resulting isotactic/atactic stereoblock propagation (Scheme 1).[3,4]

Scheme 1

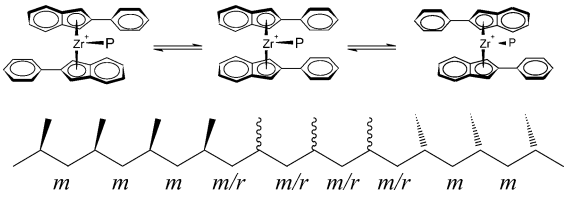

Since then, a similar polymerization behavior has been reported for a variety of bis(2-Ar-indenyl) zirconocenes and hafnocenes with different Ar substituents.[4]

A number of experimental and theoretical findings, however, are not easily accommodated in the mechanism of Scheme 1. Solution NMR studies on representative precursors detected exclusively enantiomorphous *rac*-like species in fast intercon-

† Dutch Polymer Institute.
‡ Università di Napoli "Federico II".
§ Istituto di Metodologie Chimiche, CNR.

(1) Review: Brintzinger, H. H.; Fischer, D.; Muelhaupt, R.; Rieger, B.; Waymouth, R. M. *Angew. Chem., Int. Ed. Engl.* **1995**, *34*, 1143−1170.
(2) Review: Resconi, L.; Cavallo, L.; Fait, A.; Piemontesi, F. *Chem. Rev.* **2000**, *100*, 1253−1345.
(3) Coates, G. W.; Waymouth, R. M. *Science* **1995**, *267*, 217−219.
(4) Review: Lin, S.; Waymouth, R. M. *Acc. Chem. Res.* **2002**, *35*, 765−773.
(5) Petoff, J. L. M.; Agoston, T.; Lal, T. K.; Waymouth, R. M. *J. Am. Chem. Soc.* **1998**, *120*, 11316−11322.

10.1021/ja0284557 CCC: $25.00

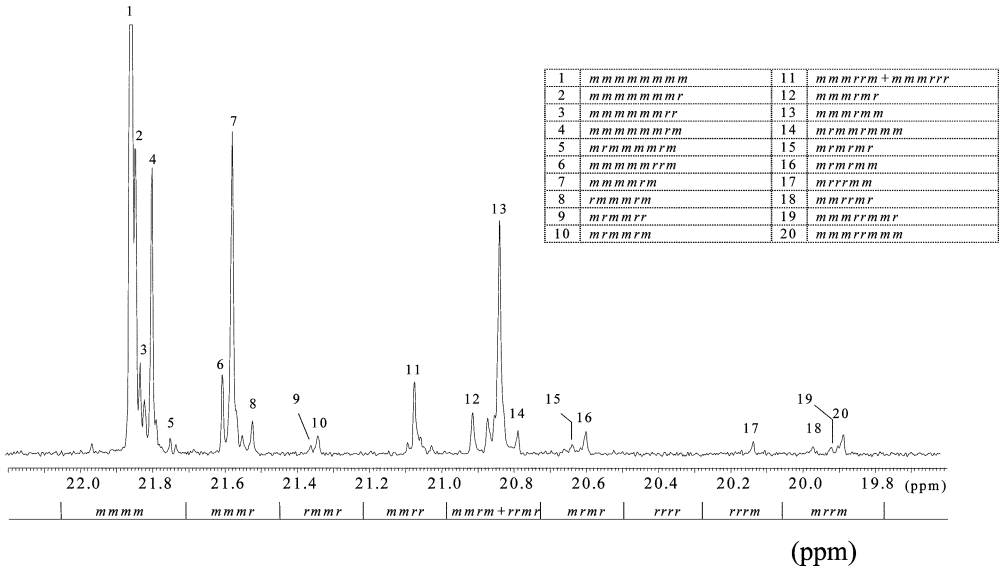

Figure 1. Methyl region of the 150 MHz ^{13}C NMR spectrum (in tetrachloroethane-1,2-d_2 at 90 °C) of polypropylene sample **PP1**. The chemical shift scale is in ppm downfield of tetramethylsilane; the assignment is based on ref 13b.

version (at 20 °C, ca. 7×10^3 ligand rotations s^{-1} for the dibenzyl complex with Ar = phenyl and ca. 70 s^{-1} for that with Ar = 3,5-di-*tert*-butylphenyl, to be compared with typical *average* polymerization rates of 10−100 propene insertions s^{-1} at the same temperature and $[C_3H_6]$ = 1−10 mol/L).[4,6] As a matter of fact, according to computer modeling[7,8] the *meso*-like conformation is less stable than the *rac*-like one, the more so the bulkier the Ar substituents, and in all cases the rotational barrier is low (2−5 kcal/mol). Last but not least, the polymerization products often have rather broad molecular mass distributions and can be solvent-separated in fractions largely differing in stereoregularity, from completely amorphous (though not purely atactic) to highly crystalline (though not completely isotactic);[4,9] this strongly suggests the coexistence of different catalytic species, possibly in equilibrium but with average lifetimes longer than the average chain growth time.

A decisive tool to face this challenging mechanistic problem is microstructural polymer analysis.[10,11] When a chain reaction builds up a macromolecule, the products of consecutive propagation events are enchained not only in statistical sense but also chemically; this makes it possible to extend the determinations of chemo-, regio-, and stereoselectivity from the simple and relatively uninformative level of single constitutional or configurational units to that of sequences thereof. A linear macromolecule, in particular, is like a tape on which the complete reaction story is sequentially and permanently recorded. To know the story, of course, one needs to read the tape, which is not at all trivial, particularly with the stereosequences.

For polypropylene, the most effective tool of configurational analysis is ^{13}C NMR. Although the results are better than for any other polyolefin, the resolution is normally limited to the steric pentads (i.e., to strands of 5 consecutive monomeric units);[10,11] this is not enough to unveil a complicated mechanism like that of "oscillating" catalysis.[11,12]

In our laboratory, however, we have developed high-field (150 MHz) ^{13}C NMR techniques enabling us to go further—in favorable cases up to the undecads but more typically to the heptads/nonads.[11,13] In two recent communications,[9,14] we reported preliminary data showing that the 150 MHz ^{13}C NMR microstructure of polypropylene chains obtained with typical "oscillating" zirconocenes is inconsistent with the hypothesis of Scheme 1; in this full paper, we narrate the whole "story" as we could read it. It is fairly complicated, and the question in the title reveals some residual margins of doubt on the conclusion; anyhow, we find it a good story.

Results and Discussion

Sterically Hindered Catalyst [(2-(3,5-di-*tert*-Butyl-4-methoxyphenyl)indenyl)$_2$ZrP]$^+$ (CAT1). The methyl region of the 150 MHz ^{13}C NMR spectrum of a typical polypropylene sample (**PP1**) prepared at 20 °C, $[C_3H_6]$ = 6.7 mol/L in toluene, with catalyst system (2-(3,5-di-*tert*-butyl-4-methoxyphenyl)indenyl)$_2$$ZrCl_2$/MAO (MAO = methylalumoxane) is shown in Figure 1; the normalized stereosequence distribution, as obtained by full spectral simulation, is reported in Table 1.

At a first sight, the spectrum looks like that of a predominantly isotactic polypropylene obtained under chain-end control;[11] in fact, in addition to the intense peak of the *mmmmmmmm*

(6) (a) Knüppel, S.; Fauré, J.; Erker, G.; Kehr, G.; Nissinen, M.; Froehlich, R. *Organometallics* **2000**, *19*, 1262−1268. (b) Schneider, N.; Schaper, F.; Schmidt, K.; Kirsten, R.; Geyer, A.; Brintzinger, H. H. *Organometallics* **2000**, *19*, 3597−3604. (c) Dreier, T.; Erker, G.; Froehlich, R.; Wibbeling, B. *Organometallics* **2000**, *19*, 4095−4103. (d) Wilmes, G. M.; France, M. B.; Lynch, S. R.; Waymouth, R. M. *Abstracts of Papers*, 224th National Meeting of the American Chemical Society, Boston, MA, Aug 18−22, 2002; American Chemical Society: Washington, DC, 2002.
(7) Cavallo, L.; Guerra, G.; Corradini, P. *Gazz. Chim. Ital.* **1996**, *126*, 463−467.
(8) (a) Pietsch, M. A.; Rappé, A. K. *J. Am. Chem. Soc.* **1996**, *118*, 10908−10909. (b) Maiti, A.; Sierka, M.; Andzelm, J.; Golab, J.; Sauer, J. *J. Phys. Chem. A* **2000**, *104*, 10932−10938.
(9) Busico, V.; Cipullo, R.; Segre, A. L.; Talarico, G.; Vacatello, M.; Van Axel Castelli, V. *Macromolecules* **2001**, *34*, 8412−8415.
(10) Tonelli, A. E. *NMR Spectroscopy and Polymer Microstructure: The Conformational Connection*; VCH Publishers: Deerfield Beach, FL, 1989.
(11) Busico, V.; Cipullo, R. *Prog. Polym. Sci.* **2001**, *26*, 443−533.
(12) (a) Bruce, M. D.; Waymouth, R. M. *Macromolecules* **1998**, *31*, 2707−2715. (b) Gauthier, W. J.; Collins, S. *Macromolecules* **1995**, *28*, 3779−3786.
(13) (a) Busico, V.; Cipullo, R.; Corradini, P.; Landriani, L.; Vacatello, M.; Segre, A. L. *Macromolecules* **1995**, *28*, 1887−1892. (b) Busico, V.; Cipullo, R.; Monaco, G.; Vacatello, M.; Segre, A. L. *Macromolecules* **1997**, *30*, 6251−6263. (c) Busico, V.; Cipullo, R.; Monaco, G.; Vacatello, M.; Bella, J.; Segre, A. L. *Macromolecules* **1998**, *31*, 8713−8719.
(14) Busico, V.; Cipullo, R.; Kretschmer, W. P.; Talarico, G.; Vacatello, M.; Van Axel Castelli, V. *Angew. Chem., Int. Ed.* **2002**, *41*, 505−508.

Table 1. 150 MHz ^{13}C NMR Stereosequence Distribution of Polypropylene Sample **PP1** and Best-Fit Calculated Ones in Terms of Different Stochastic Models (see Text)[a]

	fractional abundance		
		calcd	
stereosequence	exptl	CE model	ES model
mmmm	0.6446(125)	0.6735	0.6495
mmmmmm	0.5178(127)	0.5527	0.5267
mmmmmr	0.1082(30)	0.1148	0.1165
mmmr	0.1419(22)	0.1399	0.1436
mmmmrr	0.0255(20)	0.0119	0.0267
rmmr	0.0105(20)	0.0073	0.0079
mmrr	0.0342(20)	0.0145	0.0329
mmrm + *rmrr*	0.1336(20)	0.1414	0.1303
mmmrmm	0.0991(20)	0.1148	0.1025
mmmrmr	0.0147(22)	0.0119	0.0116
rmrm	0.0162(20)	0.0145	0.0143
mrmrmm	0.0098(20)	0.0119	0.0102
rrrr	0.0009(20)	0.0001	0.0005
rrrm	0.0045(20)	0.0015	0.0053
mrrm	0.0145(20)	0.0073	0.0156
mmrrmr	0.0029(20)	0.0012	0.0028
mmrrmm	0.0116(20)	0.0060	0.0127
		$\chi_{red}^2 = 17$	$\chi_{red}^2 = 1.3$
		$P_m = 0.906(5)$	$\sigma = 0.985(1)$
			$P_{osc} = 0.086(1)$

[a] Adjustable parameters: P_m = probability to generate a *meso* diad; σ = probability to select a given monomer enantioface at an active species of given chirality; P_{osc} = probability of enantiomorphic sites interconversion ("oscillation").

Chart 1

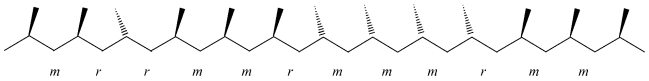

nonad, comparatively strong ones corresponding to the *mmmmmmmr*, *mmmmmmrm*, (*m*)*mmmmrm*(*m*), and (*m*)*mmmrmm*(*m*) nonads in ca. 1:1:1:1 ratio indicate that the predominant stereodefects are of ···*mmmmrmmmm*··· type.

However, the best-fit stereosequence distribution calculated in the framework of the classical Bovey's chain-end (CE) model,[15] assuming a Bernoullian distribution of the steric diads ($[m] = P_m$; $[r] = P_r = 1 - P_m$), is not satisfactory (3rd column of Table 1), as shown by the very high value of the reduced-χ^2 function ($\chi_{red}^2 = 17$). The main source of disagreement is the systematic tendency of the model to underestimate the $m_x rrm_y n$ads, which are diagnostic of (lower amounts of) ···*mmmmrrmmmm*··· stereodefects typical of site control;[11] this clearly points to the isotactic-stereoblock chain microstructure of Chart 1. Each block is the result of site control at an intrinsically chiral catalytic species and as such may contain *rr*-type stereodefects; the isolated *r* diads are junctions between stereoblocks of opposite relative configurations, formed in consequence of an inversion of chirality of the catalytic species during chain propagation.

A simple mechanism accounting for this, and also nicely in line with the aforementioned results of solution NMR[4,6] and computer modeling[7,8] catalyst studies, entails the direct interconversion of the two minimum-energy enantiomorphous *rac*-like conformations, as shown in Scheme 2.[14,16]

Chain propagation can be described in terms of the well-known enantiomorphic sites (ES) model[11,17] in its Coleman–Fox version.[18] The model has two adjustable parameters:

Scheme 2

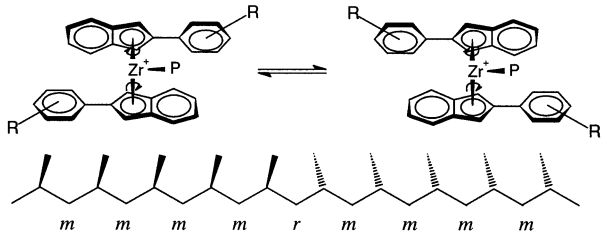

σ = probability that the monomer inserts with a given enantioface at an active center of given chirality (of course, $\sigma_1 = 1 - \sigma_2$);

P_{osc} = probability of site interconversion ("oscillation").

The 4 × 4 stochastic matrix of the propagation states and reference to the matrix multiplication codes used to generate the stereosequence distribution are given in the Methods section. The agreement with the experimental data is very good (last column of Table 1; $\chi_{red}^2 = 1.3$), for best-fit values of $\sigma = 0.985$ and $P_{osc} = 0.086$. The number average stereoblock length is $<L_{iso}> = (1 - P_{osc})/P_{osc} \approx 12$ monomeric units.

Understandably, P_{osc}—and therefore $<L_{iso}>$—depend on propene concentration (whereas σ does not). As an example, on a sample (**PP2**) prepared at $[C_3H_6] = 1.5$ mol/L we measured $P_{osc} = 0.17$, corresponding to $<L_{iso}> \approx 5$ monomeric units. Theoretically, for $[C_3H_6] \rightarrow 0$ P_{osc} tends asymptotically to 0.5 (in other words, monomer insertion and site "oscillation" tend to the same conditional probability); this limit corresponds to perfectly atactic propagation (irrespective of the value of σ).

A puzzling element of complication is that the polymers obtained can be solvent-fractionated on the basis of the degree of stereoregularity, which is, in theory, incompatible with a single-center homogeneous catalyst nature. In Table 2, we give the results of a sequential Kumagawa extraction of sample **PP1** with boiling diethyl ether, hexane, and heptane and of the ^{13}C NMR, DSC, and GPC characterization of the fractions.

The microstructural analysis shows that the increase in isotacticity of the fractions with increasing boiling point of the extracting solvent is due to a corresponding decrease of P_{osc} (i.e., increase of $<L_{iso}>$), whereas σ is invariant; this indicates that the ratio between the rates of monomer insertion and catalyst "oscillation" is broadly distributed throughout the population of active centers. The polydispersity of the raw sample is also higher than that of a Schultz–Flory distribution[19] ($M_w/M_n = 2.7$ instead of 2.0). One can think of several possible explanations, some of which of trivial physical origin (e.g., local monomer concentration gradients due to diffusion limitations, consequent to inadequate reactor stirring and/or to partial polymer precipitation and catalyst heterogenization); we note, however, that we did not observe similar deviations on polypropylene samples obtained in our laboratory with much more active and stereoselective *ansa*-metallocene catalysts. We will come back to this point later on.

"Less-Hindered" Catalyst [(2-Phenylindenyl)$_2$ZrP]$^+$ (CAT2). If a sterically hindered [(2-Ar-indenyl)$_2$ZrP]$^+$ cation

(15) Bovey, F. A.; Tiers, G. V. D. *J. Polym. Sci.* **1960**, *44*, 173–182.
(16) A similar mechanism was proposed for [((2-Me-5-isopropylcyclohexyl)-Cp)$_2$ZrP]$^+$: Kaminsky, W.; Buschermoehle, M. In *Recent Advances in Mechanistic and Synthetic Aspects of Polymerization*; Fontanille, M., Guyot, A., Eds.; Reidel: New York, 1987; pp 503–514.
(17) Shelden, R. A.; Fueno, T.; Tsunetsugu, T.; Furukawa, J. *J. Polym. Sci., Polym. Lett. Ed.* **1965**, *3*, 23.
(18) Coleman, B. D.; Fox, T. G. *J. Chem. Phys.* **1963**, *38*, 1065–1075.
(19) Flory, P. J. *Principles of Polymer Chemistry*; Cornell University Press: Ithaca, NY, 1953.

Table 2. Results of Boiling Solvent Fractionation of Polypropylene Sample **PP1** and of the Characterization of All Fractions by Means of ^{13}C NMR, DSC, and GPC

fraction[a]	wt %	[*mmmm*]	σ[b]	P_{osc}[b]	T_m[c,d] (°C)	Δh_m[c] (J/g)	M_n(kDa)	M_w/M_n
EE-soluble	7	0.579	0.987(1)	0.115(1)	Am.(e)	Am.(e)	99	2.0
EE-insoluble/ C6-soluble	40	0.591	0.984(1)	0.106(1)	78	11	208	2.0
C6-insoluble/ C7-soluble	29	0.656	0.984(1)	0.081(1)	135	11	200	1.9
C7-insoluble	24	0.736	0.98(1)	0.046(2)	141	57	285	2.0

[a] EE = diethyl ether, C6 = hexane, and C7 = heptane. [b] σ = probability to select a given monomer enantioface at an active species of given chirality; P_{osc} = probability of site interconversion ("oscillation"), according to the ES model. [c] Measured on the 2nd heating scan. [d] Maximum of the DSC melting endotherm. [e] Amorphous.

Table 3. 150 MHz ^{13}C NMR Stereosequence Distribution of Polypropylene Sample **PP3** and Best-Fit Calculated Ones in Terms of Different Stochastic Models (See Text)[a]

	fractional abundance		
		calcd	
stereosequence	exptl	ES model	ES + ISO model
mmmm	0.1426(34)	0.1245	0.1449
mmmmmm	0.0781(44)	0.0440	0.0732
mmmmmr	0.0540(20)	0.0601	0.0528
mmmr	0.1510(28)	0.1702	0.1562
rmmr	0.0609(20)	0.0581	0.0571
mmrr	0.1146(20)	0.1164	0.1147
mmrm + rmrr	0.2420(51)	0.2495	0.2400
mmmrmr	0.0359(51)	0.0410	0.0381
rmrm	0.1215(22)	0.1161	0.1144
rrrr	0.0296(20)	0.0273	0.0311
rrrrrr	0.0055(20)	0.0045	0.0056
rrrm	0.0799(20)	0.0797	0.0844
mrrm	0.0579(20)	0.0582	0.0573
mmrrmr	0.0317(20)	0.0280	0.0280
mmrrmm	0.0171(20)	0.0205	0.0190
		$\chi_{red}^2 = 12.6$	$\chi_{red}^2 = 2.5$
		$\sigma = 0.941(35)$	$\sigma = 0.991(8)$
		$P_{osc} = 0.379(19)$	$P_{osc} = 0.421(4)$
			$w_{ES} = 0.960(3)$

[a] Adjustable parameters: σ = probability to select a given monomer enantioface at an active species of given chirality; P_{osc} = probability of site interconversion ("oscillation"); w_{ES} = mixing coefficient of the ES model in the linear combination.

like **CAT1** "oscillates" between the two enantiomorphous *rac*-like conformations at an average frequency which is only slightly lower than that of propene insertion even at high $[C_3H_6]$, it is difficult to imagine that less-hindered ones can be slower than that. As a matter of fact, as already noted in the Introduction, Waymouth et al. very recently reported[6d] that at 20 °C ligand rotation for (2-phenylindenyl)$_2$ZrBz$_2$ (Bz = benzyl) is ca. 100 times faster than for (2-(3,5-di-*tert*-butylphenyl)indenyl)$_2$ZrBz$_2$. This means that for an active cation like **CAT2** P_{osc} should be predicted to be always close to 0.5 (i.e., chain propagation should be nonstereoselective).

Therefore, we were not at all surprised to find out that polypropylene samples obtained with catalyst system (2-phenylindenyl)$_2$ZrCl$_2$/MAO at 20 °C are almost completely amorphous and "atactic-like", whatever the value of $[C_3H_6]$. The 150 MHz ^{13}C NMR stereosequence distribution of one such sample (**PP3**), prepared at $[C_3H_6] = 6.7$ mol/L in toluene, is reported in Table 3. The sample deviates from perfect atacticity for a slight enrichment in *m* diads ([*m*] = 0.57). The experimental configuration is decently reproduced by the ES model for best-fit values of $\sigma = 0.94$ and $P_{osc} = 0.38$ (compare the 2nd and 3rd columns of Table 3), with the notable exception of the *mmmmmm* heptad, which is largely underestimated; this suggests that the sample contains a low "extra" amount of "long" (vide infra) isotactic sequences. Accordingly, a much better fit was obtained when the ES model was linearly combined with a second one accounting for isotactic propagation ($\sigma = 1$, $P_{osc} = 0$); the best-fit value of the mixing coefficient was $w_{ES} = 0.96$ (last column of Table 3; of course, $w_{ISO} = 1 - w_{ES} = 0.04$). What "long" means, referred to the isotactic sequences, is impossible to say from the data of Table 3, due to the "short sight" of ^{13}C NMR; any length in excess of ≈10 monomeric units gives the same numerical agreement.

Decreasing monomer concentration led, plausibly, to a further slight increase of P_{osc} and also to a decrease of w_{ISO}. As an example, on a sample (**PP4**) prepared at $[C_3H_6] = 1.5$ mol/L we measured $P_{osc} = 0.44$ and $w_{ISO} = 0.02$.

All this raises (at least) two questions:

(i) What is the origin of the isotactic sequences?

(ii) Why do our results differ from previous literature ones,[3,4] reporting a substantially higher isotactic content in polypropylene samples obtained with the same **CAT2** under (seemingly) comparable conditions?

Let us consider the latter first. The active species of a metallocene catalyst is obtained by reacting a precursor (usually a dichloride complex) with a suitable cocatalyst, which changes it into a metallocene−alkyl cation and generates correspondingly an anion which must be poorly coordinating.[1,2,20] Most typically, the cocatalyst is methylalumoxane (MAO), formally a polymer of formula $-[Al(Me)-O]_n-$ resulting from the reaction of $AlMe_3$ and H_2O in equimolar amounts. In reality, MAO is an ill-defined system containing oligomeric alumoxane structures in equilibrium with $AlMe_3$;[21] the average molar mass and the amount of "free" $AlMe_3$ depend significantly on the method of preparation, and commercial MAO solutions in toluene can differ significantly in both respects. To further complicate the picture, in some cases MAO is "modified" with the addition of a longer-chain Al−trialkyl (such as Al(isobutyl)$_3$ or Al(octyl)$_3$) to give a so-called MMAO with increased solubility in hydrocarbons and improved shelf life.

The performance of a given metallocene catalyst can be critically dependent, inter alia, on the specific MAO or MMAO used to activate the precursor, at least as far as the productivity is concerned. According to Waymouth et al.,[22] not only the productivity but also the stereoselectivity in propene polymerization of (2-phenylindenyl)$_2$ZrCl$_2$ depends on the specific MAO

(20) Review: Chen, E. Y.-X.; Marks, T. J. *Chem. Rev.* **2000**, *100*, 1391−1434.
(21) See, e.g.: (a) Babushkin, D. E.; Brintzinger, H. H. *J. Am. Chem. Soc.* **2002**, *124*, 12869−12873 and references therein. (b) Hansen, E. W.; Blom, R.; Kvernberg, P. O. *Macromol. Chem. Phys.* **2001**, *202*, 2880−2889. (c) Ystenes, M.; Eilertsen, J. L.; Liu, J.; Ott, M.; Rytter, E.; Støvneng, J. A. *J. Polym. Sci., Part A* **2000**, *38*, 3106−3127.
(22) Petoff, J. L. M.; Myers, C. L.; Waymouth, R. M. *Macromolecules* **1999**, *32*, 7984−7989.

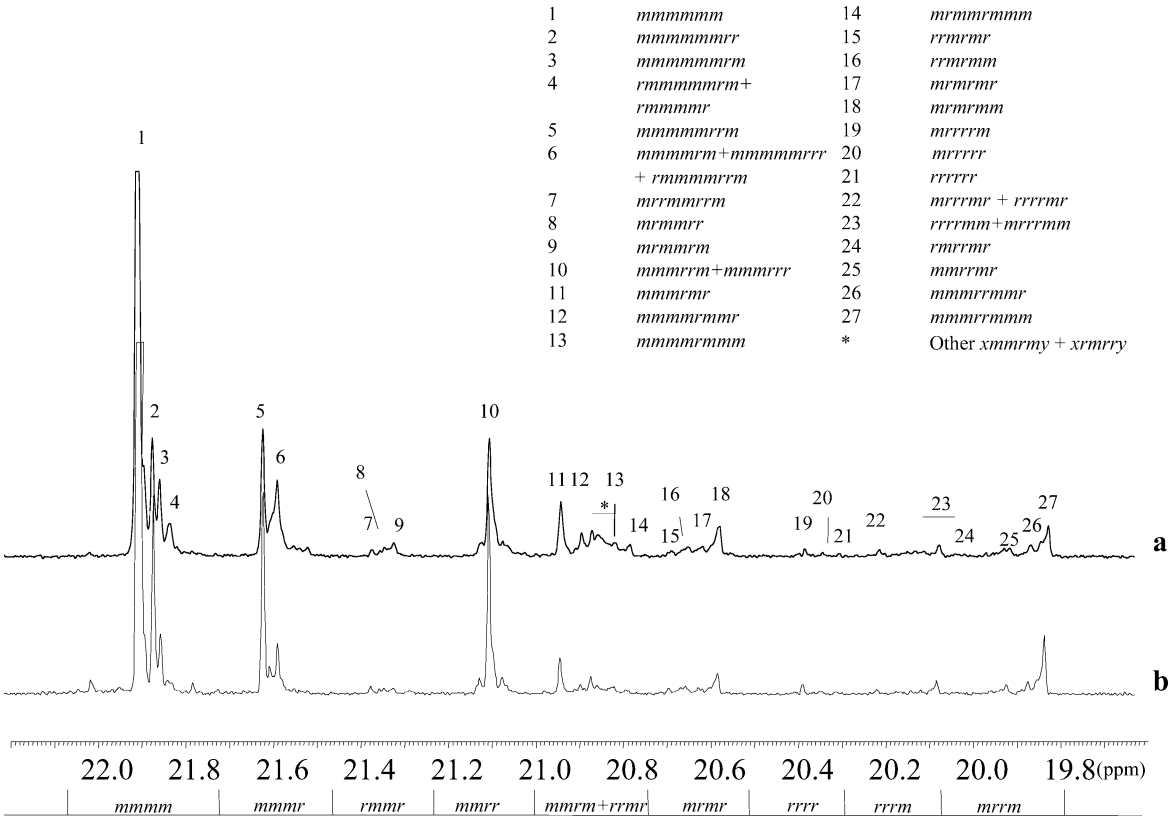

Figure 2. Methyl region of the 150 MHz ^{13}C NMR spectra (in tetrachloroethane-1,2-d_2 at 90 °C) of the semicrystalline fractions of polypropylene samples **PP5** (trace a) and **PP6** (trace b). The chemical shift scale is in ppm downfield of TMS. Peak attributions are based on ref 13b; weak unresolved resonances centered on the *mmrm* and *rmrr* pentads are marked with an asterisk.

or MMAO used to activate it. In particular, they obtained practically amorphous polymers with cocatalysts rich in "free" $AlMe_3$, whereas the controlled addition of Al(isobutyl)$_3$ to either MAO or MMAO led to a substantial increase in isotactic content and crystallinity.

To explore this cocatalyst effect, we polymerized propene under conditions identical to those used to prepare sample **PP4** but adding Al(isobutyl)$_3$ (up to 25 mol %) to our MAO (a 10% w/w solution in toluene produced by Crompton Co., containing ca. 20% of Al in the form of "free" $AlMe_3$) or replacing it with a modified MAO (MMAO-12 by Akzo Nobel BV). Both samples (**PP4-1** and **PP4-2**), however, turned out to have the same microstructure of **PP4** (within error limits; [*mmmm*] = 0.15 ± 0.01).

Rather then insisting with additional MAO types or modifications, we decided to try a better-defined alternative, i.e., $[HMe_2NC_6H_5][B(C_6F_5)_4]$ in combination with Al(isobutyl)$_3$.[1,20] To our surprise, at the ^{13}C NMR characterization the polypropylenes obtained were invariably found to be much more isotactic than those produced with MAO, independently of the Al/B ratio (see Methods section). As an example, on a sample (**PP5**) prepared at 20 °C and $[C_3H_6]$ = 6.7 mol/L in toluene we measured [*mmmmmm*] = 0.215, instead of [*mmmmmm*] = 0.078 for the corresponding sample **PP3**. From the value of M_w/M_n = 3.3 we presumed a possible microstructural dishomogeneity; as a matter of fact, by Kumagawa extraction with boiling diethyl ether, we separated a completely amorphous fraction (**PP5-am**; $M_n = 8.0 \times 10^4$ Da, $M_w/M_n = 2.1$), representing 79 wt %, from a semicrystalline one (**PP5-cryst**; $M_n = 2.0 \times 10^5$ Da, M_w/M_n = 2.5). On the latter, we measured by DSC and X-ray diffraction a melting temperature of 132 °C (2nd heating scan) and a crystallinity of 42%.

Table 4. 150 MHz ^{13}C NMR Stereosequence Distribution of Polypropylene Fraction **PP5-am**

stereosequence	fractional abundance	stereosequence	fractional abundance
mmmm	0.1815(20)	*mrmrmm*	0.0312(20)
mmmmmm	0.0975(20)	*rrrr*	0.0296(20)
mmmr	0.1548(20)	*mrrrrr*	0.0143(20)
mmmmrr	0.0446(63)	*rrrrrr*	0.0055(20)
rmmr	0.0506(20)	*rrrm*	0.0758(20)
mmrr	0.1216(20)	*rmrrmr*	0.0090(20)
mmrm + *rmrr*	0.2178(21)	*mmrrmr*	0.0298(20)
mmmrmr	0.0359(20)	*mmrrmm*	0.0225(20)
rmrm	0.1035(20)		

Both fractions were characterized by 150 MHz ^{13}C NMR. **PP5-am** turned out to be rather similar to (raw) sample **PP3**, although with slightly higher fractional abundances of the *mmmm* pentad and the *mmmmmm* heptad (compare the stereosequence distributions in Tables 4 and 3, respectively).

The spectrum and the stereosequence distribution of **PP5-cryst** can be found instead in Figure 2 (trace a) and Table 5.

To a specialist, the methyl resonance is highly informative already on inspection. The strong peak of the *mmmmmm* heptad, along with those of the *mmmmmmrr*, *mmmmmrrm*, (*m*)*mmmrrm*(*m*), and *mmmrrmmm* nonads in approximately 2:2:2:1 integral ratios, reveals a predominance of fairly long, site-controlled isotactic sequences. Relatively weak and broad multiplets in the regions of the *rmmr*, *mmrm* + *rmrr*, *rmrm*, *rrrr*, and *rrrm* pentads, with integrals in approximate ratios of 1:4:2:1:2, indicate the presence of lower amounts of atactic or

Table 5. 150 MHz ^{13}C NMR Stereosequence Distribution of Polypropylene Fraction **PP5-cryst** and Best-Fit Calculated Ones in Terms of Different Stochastic Models (See Text and Schemes 3 and 4)

	fractional abundance			
		calcd		
stereosequence	exptl	ES + ISO model	"*rac* ↔ *meso*" model	"locked-*rac*" model
mmmm	0.7249(48)	0.7230	0.7259	0.7273
mmmmmm	0.6569(88)	0.6627	0.6545	0.6545
mmmr	0.0820(20)	0.0810	0.0823	0.0827
mmmmrr	0.0486(33)	0.0418	0.0475	0.0491
rmmr	0.0091(20)	0.0095	0.0077	0.0073
mmrr	0.0575(20)	0.0623	0.0589	0.0582
mmrm + rmrr	0.0513(20)	0.0532	0.0531	0.0506
mmmrmr	0.0179(20)	0.0100	0.0109	0.0179
rmrm	0.0264(20)	0.0167	0.0190	0.0244
mrmrmm	0.0139(20)	0.0079	0.0080	0.0156
rrrr	0.0060(20)	0.0065	0.0068	0.0062
rrrm	0.0114(20)	0.0179	0.0193	0.0167
rmrrmr + mmrrmr	0.0097(20)	0.0102	0.0077	0.0061
mmrrmm	0.0217(20)	0.0197	0.0193	0.0204
		$\chi_{red}^2 = 6.5$	$\chi_{red}^2 = 5.5$	$\chi_{red}^2 = 1.3$
		$\sigma = 0.865(14)$	$\sigma = 0.980(2)$	$\sigma = 0.999(1)$
		$P_{osc} = 0.052(9)$	$P_a = 0$	
		$w_{ES} = 0.47(3)$	$P_b = 0.036(10)$	$P_{iso/ata} = 0.067(3)$
			$P_c = 0.102(33)$	$P_{ata/iso} = 0.319(15)$

"quasi-atactic" sequences, whose insolubility in the boiling solvent proves that they are chemically bound to the isotactic ones. The three remaining sharp peaks corresponding to the *mmmmmmrm* nonad and to the *mmmrmr* and *mmrmrm* heptads can be attributed specifically to junctions between isotactic and atactic blocks; their relatively high intensity suggests that the latter are *very* short (a few monomeric units). This implies that the linear combination of models used to reproduce the microstructure of sample **PP3** cannot work well here because it does not generate such junctions.

The calculation actually ended up with a poor fit ($\chi_{red}^2 = 6.5$) and unrealistic values of the adjustable parameters (3rd colum of Table 5) due to the fact that the minimization routine tried to mimic—unsuccessfully—the junction *n*ads with stereodefects of the ES propagation.

A precondition for the rational implementation of a better model is to find an answer to the embarassing question on the mechanistic origin of the isotactic sequences. There is little doubt on that these are due to *rac*-like active centers; the real problem is to understand how, for only part of the catalytic species (or, possibly, of the lifetime of each of them), a given enantiomer can keep its configuration for long enough to produce whole chains with a predominantly isotactic structure, which can be solvent-separated from the majority of stereoirregular ones.

In a nonpolar medium like toluene, the concentration of "naked" metallocene cations is virtually zero, and contact ion pairs coexist with monomer-separated and solvent-separated ones.[20,23] Let us then suppose that for part of these ion couples the mutual arrangement of the two charged moieties is such that for steric reasons the indenyl rings cannot rotate and are "locked" in the stable *rac*-like conformation; if that is the case, increasing the polarity of the solvent should affect the stereoselectivity. To check this guess, we carried out comparative propene polymerization runs with catalyst system (2-phenylindenyl)$_2$ZrCl$_2$/[HMe$_2$NC$_6$H$_5$][B(C$_6$F$_5$)$_4$]/Al(isobutyl)$_3$, used under identical conditions in toluene ($\epsilon = 2.38$) and a halogenated aromatic hydrocarbon such as bromobenzene ($\epsilon = 5.40$) or 1,2-dichlorobenzene ($\epsilon = 9.93$). Propene concentration in the liquid phase was kept well below that of the solvent (to enhance the effect of the latter), and its partial pressure adjusted to compensate for the different solubility in the various solvents (see Methods section).

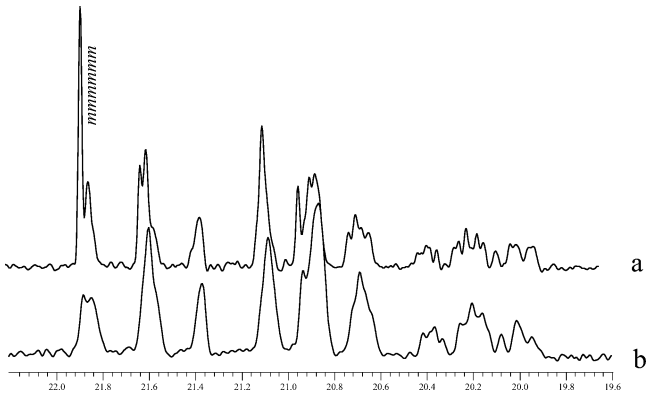

Figure 3. Methyl region of the 50 MHz ^{13}C NMR spectra (in tetrachloroethane-1,2-d_2 at 120 °C) of polypropylene samples **PP6** (trace a) and **PP7** (trace b). The chemical shift scale is in ppm downfield of TMS.

As an example, in Figure 3 we compare the methyl region of the ^{13}C NMR spectra of two polypropylene samples prepared at 20 °C and [C$_3$H$_6$] = 1.1 mol/L, one in toluene (**PP6**, trace a) and the other in bromobenzene (**PP7**, trace b). The former shows an intense peak of the isotactic *mmmmmm* heptad ([*mmmmmm*] = 0.13), which explains its semicrystallinity (T_m = 134 °C) and partial insolubility in boiling diethyl ether (6 wt %). The latter, instead, is the spectrum of a "quasi-atactic" polypropylene ([*mm*] = 0.30, [*mr*] = 0.49, [*rr*] = 0.21; [*mmmm*] = 0.09, [*mmmmmm*] ≈ 0.04), and the sample indeed turned out to be totally amorphous and diethyl ether-soluble. Similar results were

(23) See, e.g.: (a) Beck, S.; Lieber, S.; Schaper, F.; Geyer, A.; Brintzinger, H. H. *J. Am. Chem. Soc.* **2001**, *123*, 1483−1489. (b) Zhou, J.; Lancaster, S. J.; Walker, D. A.; Beck, S.; Thornton-Pett, M.; Bochmann, M. *J. Am. Chem. Soc.* **2001**, *123*, 223−237. (c) Schaper, F.; Brintzinger, H. H. In *Organometallic Catalysts and Olefin Polymerization*; Blom, R., Follestad, A., Rytter, E., Tilset, M., Ystenes, M., Eds.; Springer-Verlag: Berlin, 2001; pp 46−62. (d) Xu, Z.; Vanka, K.; Firman, T.; Michalak, A.; Zurek, E.; Zhu, C.; Ziegler, T. *Organometallics* **2002**, *21*, 2444−2453. (e) Nifant'ev, I. E.; Ustynyuk, L. Y.; Laikov, D. N. *Organometallics* **2001**, *20*, 5375−5393. (f) Lanza, G.; Fragalà, I. L.; Marks, T. J. *J. Am. Chem. Soc.* **2000**, *122*, 12764−12777.

Table 6. ^{13}C NMR Fractional Abundance of Isotactic Sequences in Polypropylene Samples Prepared with Catalyst $[(2\text{-Phenylindenyl})_2ZrP]^+$ at 20 °C

sample	cocatalyst	solvent	$[C_3H_6]$ (M)	[*mmmm*]	[*mmmmmm*]
PP4	MAO	toluene	1.5	0.114	0.049
PP3	MAO	toluene	6.7	0.143	0.078
PP6	borate/TIBAl[a]	toluene	1.1	0.18	0.13
PP7	borate/TIBAl[a]	BrBz[b]	1.1	0.09	0.04
PP5	borate/TIBAl[a]	toluene	6.7	0.295	0.215

[a] $[HMe_2NC_6H_5][B(C_6F_5)_4]$/Al(iso*butyl*)$_3$. [b] Bromobenzene.

Scheme 3

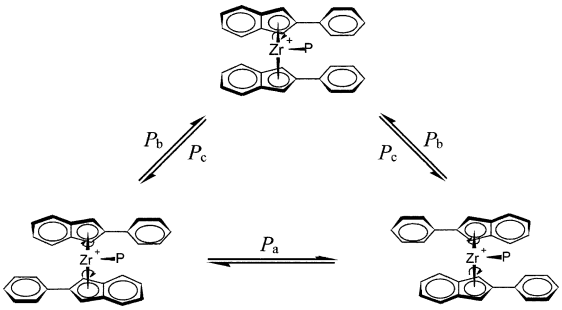

obtained in 1,2-dichlorobenzene.[14] In Table 6 we summarize our observations; in our opinion, the fact that **CAT2** generates appreciable amounts of crystallizable isotactic sequences only in a nonpolar solvent, and particularly with a $[HMe_2NC_6H_5]$-$[B(C_6F_5)_4]$/Al(isobutyl)$_3$ cocatalyst, is consistent with the hypothesis of a cation/anion "interlocking" as a source of stereorigidity (although it is not enough to prove it). If that is the case, isotactic chain propagation for this catalyst, at odds with **CAT1**, should be regarded more as an "accident" than as an intrinsic feature. From here on, we will refer to this as the "locked-*rac*" hypothesis.

As an alternative, Lin and Waymouth recently reformulated the mechanism of Scheme 1 as shown in Scheme 3:[4,24] the catalyst can "oscillate" either between the two enantiomorphous *rac*-like conformations, with a conditional probability P_a, or to and from each of these and the *meso*-like conformation, with conditional probabilities P_b and P_c. Their "*rac* ↔ *meso*" hypothesis traces "quasi-atactic" propagation to the *meso*-like conformation, when accessible (for sterically hindered cations such as **CAT1**, they agreed with us that $P_b \approx 0$, $P_c \approx 1$).

With this in mind, we can go back now to polypropylene fraction **PP5-cryst** (Figure 2 and Table 5) and resume the search for a stochastic model of chain propagation able to reproduce its microstructure. If we accept the "*rac* ↔ *meso*" hypothesis of Scheme 3, the corresponding Coleman−Fox model requires a 6×6 matrix of propagation states (see Methods section) and four adjustable parameters: one for the enantioselectivity of the two enantiomorphous *rac*-like species (σ) and the three conditional probabilities of "oscillation" (P_a, P_b, and P_c). The best-fit stereosequence distribution is reported in Table 5 (4th column); the χ_{red}^2 test indicates a rather poor match with the experiment, and in fact the *mmmrmr* and *mmrmrm* heptads are largely underestimated, whereas the *rrrm* pentad is largely overestimated. The solution has $\sigma = 0.98$ and $P_a = 0$ (which means that the only communication between the two *rac*-like species would be via the *meso*-like one) and $P_b = 0.04$ and $P_c = 0.10$ (from which one can estimate the average lengths of the isotactic and atactic blocks, $<L_{iso}> = (1 - P_b)/P_b \approx 25$ monomeric units, $<L_{ata}> = (1 - 2P_c)/2P_c \approx 4$ monomeric units).

Chart 2

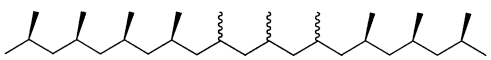

Scheme 4

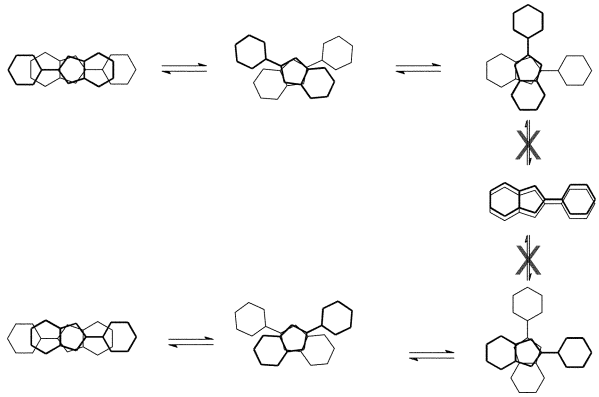

Importantly, upon scanning through our library of chain propagation models, we discovered—somewhat unexpectedly—that a very good agreement with the experimental data can be achieved instead with a simple Coleman−Fox model involving only *two* interconverting centers (one stereoselective due to site control and the other nonstereoselective) and three adjustable parameters: the enantioselectivity of the former center (σ) and the two probabilities of interconversion ($P_{iso/ata}$ and $P_{ata/iso}$). The corresponding 4×4 matrix of the propagation states is given in the Methods section ($\mathbf{M}_{LR}$). The best-fit values of such parameters are $\sigma \approx 1$, $P_{iso/ata} = 0.07$, and $P_{ata/iso} = 0.32$, and the χ_{red}^2 value is as low as 1.3 (last column of Table 5). This solution corresponds to the chain microstructure shown in Chart 2: a sequence of fairly long ($<L_{iso}> = (1 - P_{iso/ata})/P_{iso/ata} \approx$ 13 monomeric units) isotactic blocks *with the same relative configuration*, separated by a few (*on average*, between 2 and 3) stereoirregular units. The conclusion is that the isotactic-selective center shortly loses and resumes the stereocontrol *without inverting its configuration*, and the necessary implication is that the nonstereoselective center is *not* a *meso*-like species, because there is no reason the latter should return to only one of the two *rac*-like species (Scheme 3).

The said microstructure, on the other hand, is compatible with our "locked-*rac*" hypothesis, provided that one admits that the anion-induced stereorigidity is not complete. Molecular mechanics studies on model $[(2\text{-phenylindenyl})_2ZrR]^+$ cations[7] actually pointed out that the potential well of the *rac*-like conformation is rather shallow, with two close by minima differing by some 80° in the mutual orientation of the indenyl ligands, and that further rotation of one ligand leads past a low barrier to a "T-shaped" C_1-symmetric species which is only slightly higher in internal energy and nonenantioselective (Scheme 4). Restricted rotation within this well (i.e., without reaching the *meso*-like conformation) may well lead to polymer chains such as in Chart 2.

It may be worthy to note that the possibility to discriminate between the two mechanistic proposals by means of microstructural polymer analysis was due to the lucky circumstance that, in the examined case, the stereoirregular units between

(24) Wilmes, G. M.; Lin, S.; Waymouth, R. M. *Macromolecules* **2002**, *35*, 5382−5387.

Chart 3

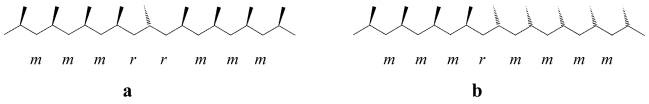

contiguous isotactic blocks were shorter than the maximum sequence length afforded by 150 MHz ^{13}C NMR.

The impact of decreasing monomer concentration on polymer microstructure is also revealing. The "*rac* ↔ *meso*" and "locked-*rac*" hypotheses agree on that the average stereoblock length should decrease, due to the decrease in the ratio between the rates of monomer insertion and catalyst "oscillation", and that the much shorter atactic sequences should be the first to "shrink" to single monomeric units; in this limit, however, the former predicts the two stereostructures a and b of Chart 3 in equimolar amounts and the latter instead stereostructure a only.

The methyl region of the 150 MHz ^{13}C NMR spectrum of the semicrystalline fraction of sample **PP6**, prepared under conditions identical to that for **PP5** but at $[C_3H_6] = 1.1$ mol/L (instead of 6.7 mol/L), is shown in Figure 2 (trace b). Compared with the homologous fraction of sample **PP5** (Figure 2, trace a), the spectrum looks more simple, although the *mmmmmm* peak has roughly the same integral (59% instead of 66%); the reason is that most residual stereodefects are indeed constituted by isolated monomeric units and that these are practically all in the form of Chart 3a—note the clear peak of the symmetrical (multiplicity = 1) *mmmrrmmm* nonad (much more intense than for **PP5**) and the substantial absence of the peak of the nonsymmetrical (multiplicity = 2) *mmmmrmmm* nonad.

Possible Hypothesis on the Nature of the Conformationally "Locked-*rac*" Species. It is difficult not to note the similarity between **CAT2** in "locked-*rac*" conformation and a bis(1-indenyl) *ansa*-metallocene cation in *rac* configuration.[1,2] The stereorigidity of the latter is ensured by a covalent interannular bridge; we are tempted to propose that, for the former, the role of the bridge is played by the counterion.

Cation/anion interaction is probably the most complicated aspect of metallocene catalysis.[1,20,23] It is generally accepted that, in the absence of monomer, a $[L_nMtR]^+$ species tends to form a contact ion pair, in which the anion is in the region of space where the monomer would be. The interaction is mainly electrostatic, but with certain anions (like borates) it can have a directional component. For a monomer molecule to insert, it is assumed that the anion must be partly displaced[23] but to where exactly is hard to say. For an *ansa*-metallocene, the presence of the bridge limits somewhat the possibilities, and the anion is probably bound to reside at the catalyst "front"; in the case of an unbridged cation, on the other hand, more options can be considered.

Just as an example, Figure 4 shows the optimized transition state structure (as obtained by quantum mechanics/molecular mechanics; see Methods section) for propene insertion at a [*rac*-(2-phenylindenyl)$_2$ZrMe][B(C$_6$F$_5$)$_4$] ion couple, in which the borate is at the catalyst "rear", more or less where the bridge of an *ansa*-metallocene would be; in this arrangement, the two coordination sites required for a Cossee-type insertion are totally free. The calculated internal energy (relative to that of the contact ion couple plus free monomer) is $E^{\#} \approx 13$ kcal/mol, which falls already at the lower limit of the typical range of experimental activation energies reported for metallocene-catalyzed propene

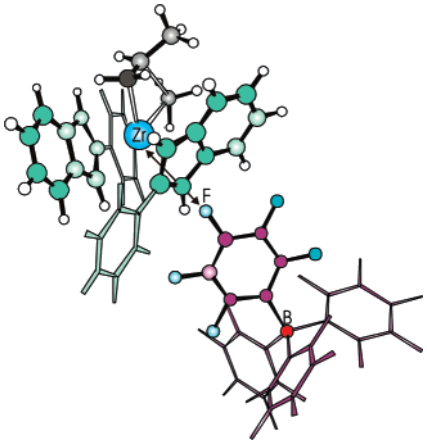

Figure 4. Quantum mechanics/molecular mechanics (QM/MM) optimized structure of the transition state for propene insertion into the Zr−Me bond of a putative [*rac*-(2-phenylindenyl)$_2$Zr(Me)][B(C$_6$F$_5$)$_4$] ion couple with the borate anion sterically interlocked at the catalyst rear (see text). The fragments treated at MM level are shown in wire frame.

polymerizations (12−18 kcal/mol).[2] On the basis of the results of similar calculations,[25] an even lower value of $E^{\#}$ can be anticipated for insertion into a longer chain. The distance between the Zr center and the nearest F atom (indicated with an arrow in Figure 4) can be as low as 0.32 nm; however, $E^{\#}$ changes by less than 2 kcal/mol for fluctuations of such a distance up to 0.40 nm. This results in the fact that 180° rotations of the sterically demanding 2-phenylindenyl moieties are hindered by the growing chain in the front and by the borate in the rear, which denies access to the *meso*-like conformation but leaves room for limited rearrangements such as that from the *rac*-like to the T-shaped conformation (Scheme 4).

Relative to more typical monomer-separated ion pairs, the structure of Figure 4 is presumably higher in free energy for entropic reasons, due to the severe conformational contraints; however, in case monomer coordination is faster than anion relocation, it may be kinetically trapped and generate stereosequences such as those in Charts 2 and/or 3a, possibly until a chain transfer event occurs. Assuming that propene coordination is stronger than that of toluene, the relative amount of "locked-*rac*" species should increase with increasing $[C_3H_6]$; this seems in line with the results in Table 6.

Although, in principle, an analogous bridging function might be played by different anions (e.g., derived from MAO), the peculiar "arrowlike" shape of $[B(C_6F_5)_4]^-$ looks particularly effective and may explain why its use with **CAT2** in nonpolar solvent resulted in polymers with a much higher content of predominantly isotactic chains than those obtained with MAO (see again Table 6).

Possible Unified Model for "Oscillating" Metallocene Catalysts. In Scheme 5 we give our comprehensive view of "oscillating" $[(2\text{-Ar-indenyl})_2ZrP]^+$ catalysts. According to us, the less stable *meso*-like conformation can be disregarded, and the active cation is "always" in *rac*-like conformation. Two dynamic regimes, however, are possible: an "oscillating" and a "locked" one. In the former, the two enantiomorphous *rac*-like conformations are in fast interconversion; the probability of "oscillation", P_{osc}, depends primarily on the bulkiness of the

(25) See, e.g.: (a) Lanza, G.; Fragalà, I. L.; Marks, T. J. *Organometallics* **2002**, *21*, 5594−5612. (b) Chan, M. S. W.; Ziegler, T. *Organometallics* **2000**, *19*, 5182−5189.

Scheme 5

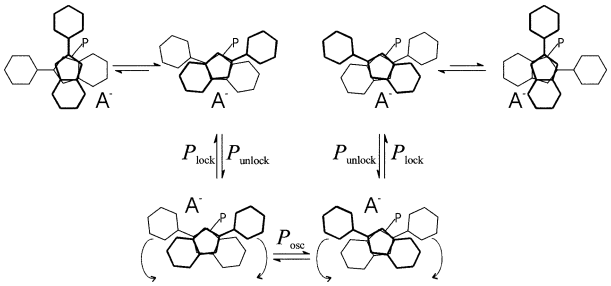

Ar substituents, on monomer concentration, and on the temperature. At 20 °C and $[C_3H_6] = 6.7$ mol/L in toluene, for **CAT1** P_{osc} is ca. 10 times lower than the probability of monomer insertion P_{ins} (in substantial agreement with dynamic NMR measurements on a closely related model complex[6d]); this results in an isotactic-stereoblock chain propagation (Scheme 2 and Chart 1). Under the same conditions, for the much more mobile[6d] **CAT2** the ratio P_{osc}/P_{ins} is ca. 1, and therefore, chain propagation is nonstereoselective.

In the "locked" regime, instead, the "oscillation" is frozen, and the active species keeps its configuration for a time long enough to produce long isotactic blocks, although with the possibility of transient distortions leading to the generation of stereoirregular units which at high $[C_3H_6]$ can occur in short sequences (Scheme 4 and Chart 2).

On the grounds of experimental and theoretical evidence, we believe that the transition from the "oscillating" to the "locked" regime is induced by the association of the active cation with a counteranion, playing a role analogous to that of the covalent bridge in an *ansa*-metallocene. For a given catalyst, the conditional probabilities of "locking" and "unlocking" (P_{lock} and P_{unlock}), and the weight fraction of polymer produced in the "locked" regime ($w_{lock} = P_{unlock}/(P_{lock}+P_{unlock})$), depend strongly on the cocatalyst and on the solvent. At 20 °C and $[C_3H_6] =$ 6.7 mol/L in toluene, for **CAT2** we measured $w_{lock} \approx 0.04$ with MAO; with $[HMe_2NC_6H_5][B(C_6F_5)_4]/Al(isobutyl)_3$, instead, w_{lock} was ≈ 0.21, and P_{unlock} was low enough to allow the production of whole predominantly isotactic macromolecules. For **CAT1**, on the other hand, it appears that the "locked" regime is of lower importance,[14] possibly due to the fact that the bulky Ar substituents make the interlocking with a counteranion more difficult.

Conclusions

The 150 MHz ^{13}C NMR microstructural analysis of polypropylene samples produced with two representative "oscillating" metallocene catalysts of largely different steric hindrance, namely $[(2\text{-}(3,5\text{-di-}tert\text{-butyl-}4\text{-methoxyphenyl})\text{indenyl})_2ZrP]^+$ and $[(2\text{-phenylindenyl})_2ZrP]^+$, led us to conclude that the original mechanistic proposal of an "oscillation" between a *rac*-like (isotactic-selective) and a *meso*-like (nonstereoselective) conformation[3] (Scheme 1) cannot explain the observed polymer configuration. The isotactic-stereoblock nature of the polymers obtained with the former catalyst (Chart 1) proves unambiguously that the active cation "oscillates" between the two enantiomorphous *rac*-like conformations (Scheme 2) at an average frequency that, even at high propene concentration, is only slightly lower than that of monomer insertion. The less hindered $[(2\text{-phenylindenyl})_2ZrP]^+$ generates a largely stereoirregular polypropylene, which is the logical consequence of a much faster ligand rotation; however, depending on the use conditions (in particular, on the nature of the cocatalyst and the polarity of the solvent), the polymerization products may also contain appreciable amounts of a fairly isotactic fraction. The peculiar microstructure of this fraction, with isotactic blocks *of the same relative configuration* spanned by very short atactic ones (Chart 2), rules out the possibility that the latter are due to an active species in *meso*-like conformation (Scheme 3) and points rather to a conformationally "locked" *rac*-like species with restricted ring mobility (Scheme 4). The hypothesis of a stereorigidity induced by the proximity to a counteranion, which would play the role of the interannular bridge in the *rac*-bis(indenyl) *ansa*-metallocenes, was tested by computer modeling on a $[rac\text{-}(2\text{-phenylindenyl})_2ZrMe(C_3H_6)][B(C_6F_5)_4]$ ion couple (Figure 4) and found viable.

Thus, it appears that these highly dynamic bis(2-Ar-indenyl) zirconocenes represent the extreme of a range of behaviors limited, to the other side, by the truly stereorigid *rac*-C_2-symmetric *ansa*-metallocenes with homotopic sites,[1,2] for which the existence of a counterion can be practically ignored as far as the microstructure of the polymer is concerned. Somewhere between are all *ansa*-metallocenes with nonequivalent sites, for which—at least in some cases—relevant counterion and solvent effects on the relative rates of monomer insertion and site epimerization (chain back-skip), and hence on the stereoselectivity, have also been documented.[26]

Methods

Propene Polymerization. The polypropylene samples were prepared in a computer-controlled stainless steel reactor (Brignole, model AU-1, internal volume 1.0 L), equipped with a magnetic stirrer (1000 rpm) and a glass vial holder-breaker. For each run, the reactor was charged with an aliquot of dry solvent (toluene (Aldrich) or bromobenzene (Aldrich) distilled over P_2O_5) containing the cocatalyst, thermostated at 20 °C, and saturated with propene (SON, polymerization grade) at the appropriate partial pressure. The reaction was started by breaking a glass vial (sealed under argon in a Vacuum Atmospheres glovebox) containing the solid catalyst (prepared according to the literature[3,27]), allowed to proceed at constant propene concentration (partial pressure) for a convenient time, and stopped by quick monomer degassing. For details on individual runs, see Table 7. All polymers were coagulated in methanol (1.0 L) added with 20 mL of HCl (aqueous, concentrated), washed with methanol, filtered off, and vacuum-dried.

^{13}C NMR Polymer Characterization and Configurational Analysis. Quantitative ^{13}C NMR spectra were recorded with a Bruker AMX-600 spectrometer operating at 150 MHz, on polymer solutions in tetrachloroethane-1,2-d_2 (10 mg/mL) at 90−110 °C, as already described.[13b,c] Each spectrum was fully simulated with the SHAPE-2000 program[28] as a convenient set of Lorentzian functions. Due to the fact that the complete fine structure at nonad/undecad level is not accessible even at 150 MHz,[11,13] part of such Lorentzians cannot be univocally and entirely associated to a specific steric *n*ad, because this would require to locate all constituting $(n + m)$ads with appreciably different values of chemical shifts (±0.002 ppm). In such cases, for the subsequent configurational analysis we used only summed areas and not the strongly correlated individual ones obtained by the complex least-squares fit; this reduced the integration error to that coming from the noise (which is very low). The statistical analysis of the stereosequence distribution was carried out with the CONFSTAT suite;[29] the

(26) See, e.g.: (a) Chen, M.-C.; Marks, T. J. *J. Am. Chem. Soc.* **2001**, *123*, 11803−11804. (b) Shiomura, T.; Asanuma, T.; Inoue, N. *Macromol. Rapid Commun.* **1996**, *17*, 9−14.
(27) Witte, P.; Lal, T. K.; Waymouth, R. M. *Organometallics* **1999**, *18*, 4147−4155.
(28) Vacatello, M. *SHAPE-2000*; University of Naples Federico II: Naples, Italy (vacatello@chemistry.unina.it).

Table 7. Details of Polypropylene Sample Preparation (See Text)

sample	catal (mg)	solvent[a] (mL)	MAO[c] (mL)	borate[e] (mg)	TIBAl[f] (mL)	$p(C_3H_6)$ (bar)	$[C_3H_6]$ (mol/L)	t (min)	yield (g)
PP1	8.1	45	5.7			9.2	6.7	60	17.1
PP2	4.1	100	2.9			2.0	1.5	60	1.2
PP3	7.0	45	7.1			9.2	6.7	60	9.2
PP4	2.3	100	2.4			2.0	1.5	60	0.64
PP4-1	3.5	150	3.6		0.25	2.0	1.5	30	0.23
PP4-2	2.4	150	0.85[d]			2.0	1.5	60	0.62
PP5	6.1	50		24	1.0	9.2	6.7	60	5.0
PP6	3.0	150		12	0.25	1.5	1.1	25	1.4
PP6-1	3.2	150		12	0.12	1.5	1.1	30	1.2
PP7	3.2	150[b]		12	0.25	1.8	1.1	30	0.47

[a] Toluene, except for **PP7**. [b] Bromobenzene. [c] Crompton Co., 10% w/w solution in toluene. [d] MMAO-12 (Akzo Nobel BV; 30% w/w solution in toluene). [e] $[HMe_2NC_6H_5)][B(C_6F_5)_4]$ (Boulder Scientific Co.). [f] Al(isobutyl)$_3$ (Crompton Co.).

principles behind the program and the matrix multiplication codes used are described in detail in refs 11 and 13a. The stochastic matrixes of propagation states for the various models are given below.

ES model:

$$\mathbf{M}_{ES} = \begin{array}{c|cc} & R & S \\ \hline R & \mathbf{I}(1-P_{osc}) & \mathbf{I}'P_{osc} \\ S & \mathbf{I}'(1-P_{osc}) & \mathbf{I}P_{osc} \end{array}$$

"*rac* ↔ *meso*" model:

$$\mathbf{M}_{RM} = \begin{array}{c|ccc} & R & S & R \quad S \\ \hline R & \mathbf{A}(1-2P_c) & \mathbf{I}P_c & \mathbf{I}'P_c \\ S & & & \\ R & \mathbf{A}P_b & \mathbf{I}(1-P_a-P_b) & \mathbf{I}'P_a \\ S & & & \\ R & \mathbf{A}P_b & \mathbf{I}P_a & \mathbf{I}'(1-P_a-P_b) \\ S & & & \end{array}$$

"Locked-*rac*" model:

$$\mathbf{M}_{LR} = \begin{array}{c|cc} & R & S \\ \hline R & \mathbf{I}(1-P_{iso/ata}) & \mathbf{A}P_{iso/ata} \\ S & & \\ R & \mathbf{A}(1-P_{ata/iso}) & \mathbf{I}P_{ata/iso} \\ S & & \end{array}$$

In the models

$$\mathbf{I} = \begin{array}{c|cc} & R & S \\ \hline R & \sigma & 1-\sigma \\ S & \sigma & 1-\sigma \end{array}$$

$$\mathbf{I}' = \begin{array}{c|cc} & R & S \\ \hline R & 1-\sigma & \sigma \\ S & 1-\sigma & \sigma \end{array}$$

$$\mathbf{A} = \begin{array}{c|cc} & R & S \\ \hline R & 0.5 & 0.5 \\ S & 0.5 & 0.5 \end{array}$$

For each model, the uncertainty on the adjustable parameters was evaluated with the Monte Carlo subroutine of CONFSTAT, changing their best-fit values at random and accepting all solutions with χ_{red}^2 values up to 1.2 times that at the absolute minimum.

Other Polymer Characterizations. DSC curves were recorded with a Perkin-Elmer DSC-7 apparatus, at the scanning rate of 10 °C/min, in flowing nitrogen. X-ray powder diffraction spectra were taken on a Philips automatic diffractometer, using Ni-filtered Cu Kα radiation. Molecular mass distributions were evaluated by gel permeation chromatography (GPC), using a Polymer Laboratories GPC220 apparatus equipped with a Viscotek 220R viscosimeter, on polymer solutions in 1,2,4-trichlorobenzene at 135 °C.

Quantum Mechanics/Molecular Mechanics (QM/MM) Modeling of the Pseudo-Transition State of Figure 4. QM/MM calculations (in the absence of solvent) were first carried out on the separate cation and anion. After full optimization, these were approached as shown in the figure, at an initial distance between the Zr atom and the *p*-F atom of the interlocked $-C_6F_5$ ring of 0.27 nm,[30] and the system was allowed to optimize with the only constraint of a 0.22 nm length for the incipient C−C bond in the four-center transition state. In all cases, stationary points on the potential energy surface were calculated with the Amsterdam density functional (ADF) program system,[31] developed by Baerends et al.[32,33] and modified by Cavallo et al.[34,35] to include standard molecular mechanics force fields in such a way that the QM and MM parts are coupled self-consistently.[36] Energetics and geometries were evaluated by using the local exchange-correlation potential by Vosko et al.,[37] augmented in a self-consistent manner with Becke's exchange gradient correction[38] and Perdew's correlation gradient correction (BP86).[39,40] The partitioning of the system into QM and MM parts involved only the phenyl substituents of the indenyl ligands and the three $-C_6F_5$ rings of the $[B(C_6F_5)_4]^-$ anion pointing away from Zr (in the QM simulation, the latter rings were represented by F atoms). A file with the atomic coordinates can be obtained from the authors.

Acknowledgment. This study was funded by the Dutch Polymer Institute (DPI Project No. 100). V.V.A.C. acknowledges the DPI for a postdoctoral fellowship. V.B., R.C., and M.V. are grateful to the Italian Ministry for University (PRIN 2000) for financial assistance. The authors thank Dr. Winfried P. Kretschmer (University Groningen) for the preparation of a sample of (2-(3,5-di-*tert*-butyl-4-methoxyphenyl)indenyl)$_2$ZrCl$_2$, Ms. Valentina Langella for carrying out part of the polymerization runs, and the Centro Interdipartimentale di Metodologie Chimico-Fisiche (University of Naples Federico II) for computational time.

JA0284557

(29) Vacatello, M. *CONFSTAT (Ver 3.1 for Windows)*; University of Naples Federico II: Naples, Italy (vacatello@chemistry.unina.it).

(30) See, e.g.: Yang, X.; Stern, C. L.; Marks, T. J. *Organometallics* **1991**, *10*, 840−842.
(31) *ADF 2.3.0*; Theoretical Chemistry, Vrije Universiteit: Amsterdam, 1996.
(32) Baerends, E. J.; Ellis, D. E.; Ros, P. *Chem. Phys.* **1973**, *2*, 41−51.
(33) te Velde, B.; Baerends, E. J. *J. Comput. Phys.* **1992**, *99*, 84−98.
(34) Cavallo, L.; Woo, T. K.; Ziegler, T. *Can. J. Chem.* **1998**, *76*, 1457−1466.
(35) Woo, T. K.; Cavallo, L.; Ziegler, T. *Theor. Chem. Acc.* **1998**, *100*, 307−313.
(36) Maseras, F.; Morokuma, K. *J. Comput. Chem.* **1995**, *16*, 1170−1179.
(37) Vosko, S. H.; Wilk, L.; Nusair, M. *Can. J. Phys.* **1980**, *58*, 1200−1211.
(38) Becke, A. D. *Phys. Rev. A* **1988**, *38*, 3098−3100.
(39) Perdew, J. P. *Phys. Rev. B* **1986**, *33*, 8822−8824.
(40) Perdew, J. P. *Phys. Rev. B* **1986**, *34*, 7406.